Matrix Metalloproteinase-9 Undergoes Expression and Activation during Dendritic Remodeling in Adult Hippocampus

Arek Szklarczyk,[1,2] Joanna Lapinska,[1] Marcin Rylski,[1,3] Ronald D. G. McKay,[2] and Leszek Kaczmarek[1]

[1]Laboratory of Molecular Neurobiology, Nencki Institute, PL-02-093 Warsaw, Poland, [2]Laboratory of Molecular Biology, National Institute of Neurological Disorders and Stroke, National Institutes of Health, Bethesda, Maryland 20892, and [3]Department of Genetics, Faculty of Biology, Warmia and Masuria University, PL-10-719 Olsztyn, Poland

Neurons of adult brain are able to remodel their synaptic connections in response to various stimuli. Modifications of the peridendritic environment, including the extracellular matrix, are likely to play a role during synapse remodeling. Proteolytic disassembly of ECM is a complex process using the regulated actions of specific extracellular proteinases. One of best-characterized families of matrix-modifying enzymes is the matrix metalloproteinase (MMP) family. Here, we describe changes in the expression and function of two well known MMPs, MMP-9 and MMP-2, in adult rat brain before and after systemic administration of the glutamate receptor agonist kainate. Kainate application results in enhanced synaptic transmission and seizures followed by selective tissue remodeling, primarily in hippocampal dentate gyrus. MMP-9 but not MMP-2 was highly expressed by neurons in normal adult rat brain. MMP-9 protein was localized in neuronal cell bodies and dendrites. Kainate upregulated the level of MMP-9 mRNA and protein within hours after drug administration. This was followed several hours later by MMP-9 enzymatic activation. Within hippocampus, MMP-9 mRNA and activity were increased selectively in dentate gyrus, including its dendritic layer. In addition, MMP-9 mRNA levels decreased in areas undergoing neuronal cell loss. This unique spatiotemporal pattern of MMP-9 expression suggests its involvement in activity-dependent remodeling of dendritic architecture with possible effects on synaptic physiology.

Key words: brain MMP-9 and MMP-2; matrix metalloproteinases; extracellular proteolysis; dendritic remodeling; hippocampus; mRNA translocation; brain extracellular matrix; kainic acid; neuronal activity-dependent gene expression

Matrix metalloproteinases (MMPs) constitute a large family of extracellular enzymes, which function to remodel the pericellular environment, primarily through the cleavage of ECM proteins (Werb, 1997). MMPs can also participate in extracellular signaling by selectively exposing hidden ECM epitopes (Nagase and Woessner, 1999). In addition, the functions of MMPs may not be limited to ECM remodeling, because these enzymes are involved in the proteolytic processing of non-ECM receptors and ligands. MMPs are activated enzymatically by conversion of a latent form (proenzyme) to an active form by propeptide processing. Once activated, the proteolytic activity of MMPs is counterbalanced by their natural inhibitors the tissue inhibitors of matrix metalloproteinases (TIMPs). MMPs expression, secretion, and activation are all controlled by various local and systemic factors (Nagase and Woessner, 1999).

Considering the importance of MMPs and TIMPs in formation and remodeling of many peripheral tissues, surprisingly little is known regarding the function of these proteins in the CNS. Prevailing data imply that MMPs are involved in glial functions. Results on MMP and TIMP localization in the CNS have been rather incoherent but do suggest that MMP expression is not specific to a given cell type (Rivera and Khrestchatisky, 1999; Jaworski, 2000). Changes in MMP expression have also been reported in various neuropathologies involving both neurons (neurodegeneration) and glial cells (inflammation and gliomas; Yong et al., 2001). These data suggest that in the brain, MMPs may be involved in a variety of cellular functions depending on the cell type involved.

Recently, it has been demonstrated that neuronal TIMP-1 is regulated by synaptic activity (Nedivi et al., 1993; Rivera et al., 1997; Jaworski et al., 1999). This prompted us to address the hypothesis that MMPs are involved in the activity-dependent reorganization of neuronal architecture.

Here, we report on the expression pattern and enzymatic activity of MMP-9 and MMP-2 in adult rat brain and address changes that these enzymes undergo during tissue remodeling triggered by kainate administration. Kainate selectively activates non-NMDA glutamate ionotropic receptors, resulting in a generalized increase in synaptic activity and seizures. As a consequence of this, selective neuronal loss and tissue reorganization, primarily in the limbic system, develop (Matthews et al., 1976a,b; Cronin and Dudek, 1988). In this study, we demonstrate that MMP-9 and MMP-2 are differentially expressed by neurons and astrocytes, respectively. Kainate administration resulted in upregulation of MMP-9 mRNA and protein as well as its enzymatic activation in hippocampal dentate gyrus. This unique spatiotemporal change in the pattern of neuronal MMP-9 expression sug-

Received Feb. 7, 2001; revised Oct. 29, 2001; accepted Nov. 6, 2001.

This work was supported by the State Committee for Scientific Research (KBN; Poland), Grant 6 P04A 081 19 (L.K. and J.L.), and was included in part in the activities of the COSTB10 action of the European Union and supported by the KBN. A.S. was supported by a Foundation for Polish Science postdoctoral fellowship. M.R. was supported by a Polish Network for Cell and Molecular Biology United Nations Education, Science, and Culture Organization-Polish Academy of Sciences fellowship. The help of S. Szymczak in preparation of isolated dentate gyri is greatly appreciated, and comments by Dr. David Owens and Joanna Mizgalska are also greatly appreciated.

Correspondence should be addressed to Dr. Arek Szklarczyk, Laboratory of Molecular Biology, National Institute of Neurological Disorders and Stroke, National Institutes of Health, 36 Convent Drive, Building 36, Room 3C09, Bethesda, MD 20892-4092. E-mail: szklarca@ninds.nih.gov.

gests its involvement in activity-dependent formation or remodeling of dendritic architecture.

MATERIALS AND METHODS

Kainate treatment. Experiments were performed using 2-month-Wistar male rats (250–300 gm) obtained from the Nencki Institute Animal Facility. Rules established by the Ethical Committee on Animal Research of the Nencki Institute and based on national laws were strictly followed.

Kainate (Sigma, St. Louis, MO; 10 mg/kg) was administered by intraperitoneal injections. To exclude effects of the injection itself, the animals were handled and injected daily with physiological saline (0.9% NaCl) for 3–4 d before the experimental treatment. After this period, rats were injected with either kainate or 0.9% NaCl and observed for up to 6 hr after injection. Only the animals displaying the characteristic pattern of limbic seizures (i.e., wet dog shakes followed by at least three attacks of stereotypic piano player behavior) that developed within 1–2 hr after kainate administration were used in these experiments (~70% of the rats). Rats were decapitated at different times after drug administration, and the brains were removed and processed as described in detail below. At least five independent experiments with seven or eight animals per time point were performed.

In situ *hybridization.* The method for *in situ* mRNA analysis followed that described by Konopka et al. (1998). Briefly, isolated brains were immediately frozen on dry ice and cut into 20 μm sections using a cryostat. Sections were fixed in 4% cold paraformaldehyde in PBS, dehydrated, and prehybridized for 2 hr at 37°C in buffer containing 50% formamide, 2× SSC (0.3 M sodium chloride and 0.03 M sodium citrate, pH 7.0), 1× Denhardt's solution (0.02% Ficoll 400, 0.02% polyvinyl pyrrolidone, and 0.02% bovine serum albumin), 200 μg/ml single-stranded DNA, and 20 mM dithiothreitol. Next, the sections were hybridized overnight in the above-described solution containing additionally 10% dextran sulfate and a ^{35}S-labeled cDNA (random primer) probe at 37°C. The fragments of human MMP-9 (400 bp from 5′ end, *Bam*HI fragment) and MMP-2 (340 bp PCR fragment covering the 1350–1800 bp region) in pBluescript KS(−) were used as the probes for *in situ* hybridization (a very kind gift from Dr. Dylan Edwards, University of East Anglia; Kossakowska et al., 1993). Sections were washed for 15 min in PBS and then for 60 min in 50% formamide and 2× SSC at room temperature. Sections were exposed against β-Max Hyperfilm (Amersham Biosciences, Piscataway, NJ) for 3–6 weeks. The autoradiograms were analyzed with the personal computer-based software VFG Pro Vision, version 1.004/88.

Nissl staining. After *in situ* hybridization, brain slices were stained with 0.1% cresyl violet (Sigma) according to the Nissl method and digitalized with VFG Pro Vision, version 1.004/88, software.

Immunohistochemistry. Isolated brains were immediately frozen on dry ice. Ten micrometer cryostat sections were fixed for 15 min in 4% paraformaldehyde in PBS. Sections were washed three times in PBS, pH 7.4, incubated 10 min in 0.3% H_2O_2 in PBS, washed twice in PBS containing Triton X-100 (0.3%; Sigma), and incubated with polyclonal anti-MMP-9 antibody 1 (Ab.1) or anti-MMP-2 (both 1:2000; Torrey Pines Biolabs) or anti-MMP-9 Ab.2 (1:500; Anawa, Zurich, Switzerland; catalog #5980-0207) for 48 hr at 4°C in PBS and 5% normal goat serum (Vector Laboratories, Burlingame, CA). Sections were washed three times in PBS containing Triton X-100 (0.3%; Sigma) and incubated with goat anti-rabbit biotinylated secondary antibody (1:500; Vector Laboratories) in PBS, Triton X-100, and 5% normal goat serum for 2 hr at room temperature. After three PBS-Triton X-100 washes, sections were incubated with avidin–biotin complex (1:1000 in PBS; Vector Laboratories) for 1 hr at room temperature and washed three times in PBS. The immunostaining reaction was developed using the glucose oxidase-DAB-nickel method. The sections were incubated in PBS with DAB (0.05%), glucose (0.2%), ammonium chloride (0.04%), and ammonium nickel sulfate (0.1%) (all from Sigma) for 5 min, and then 10% (v/v) glucose oxidase (Sigma; 10 U/ml in H_2O) was added. The staining reaction was stopped by two or three washes with PBS. The sections were dehydrated in ethanol solutions and xylene and embedded in Entellan (Merck, Darmstadt, Germany).

To prove the specificity of immunostaining with the anti-MMP-9 antibody, 1 μg of antibody in TBS was preincubated with 10 μg of recombinant rat MMP-9 (catalytic domain; Torrey Pines Biolabs) that was used to generate the antibody for 24 hr at 4°C. Preincubated antibody was used for immunohistochemistry according to the protocol described above.

Double labeling with fluophore-coupled antibodies. To identify the cell types expressing either MMP-9 or MMP-2, double fluorescent immunohistochemistry was performed. The slices were prepared as described above. In these experiments, anti-MMP-9 or anti-MMP-2 was used at a dilution of 1:500. Astrocytes were stained using a monoclonal anti-glial fibrillary acidic protein (GFAP) antibody (Sigma; 1:500), whereas neurons were stained with either monoclonal anti-neuron-specific nuclear antigen (NeuN; Chemicon, Temecula, CA; 1:500) or anti-microtubule-associated protein-2 (MAP-2; Sigma; 1:500). Pairs of primary antibodies were applied in PBS with 5% normal goat serum to stain the same brain sections. The staining was performed for 24 hr at 4°C. Immunolabeling was revealed using either anti-rabbit or anti-mouse secondary antibodies coupled to either green Alexa 488 (Molecular Probes, Eugene, OR; 1:200) or red rhodamine (Jackson ImmunoResearch, West Grove, PA; 1:500), respectively. After incubation for 2 hr at room temperature with the secondary antibodies, sections were washed in PBS, counterstained with 5 μg/ml 4′,6-diamidino-2-phenylindole (DAPI; stains cell nuclei blue) in PBS for 5 min, washed in PBS, and mounted in AquaMount (Polysciences, Warrington, PA). Digital images of green, red, and blue stainings from the same section were taken using a Spot camera and Zeiss (Thornwood, NY) microscope. Images were adjusted with Adobe (Mountain View, CA) Photoshop 5 software.

In situ *zymography.* Isolated brains were immediately frozen on dry ice. Ten micrometer cryostat sections were incubated with different substrates: gelatin-Alexa 488 conjugate or casein-Bodipy FL conjugate (panproteinase substrate) from Molecular Probes (according to the manufacturer's instruction). Sections were incubated at 37°C for 8 hr and then washed three times in water and fixed in 4% paraformaldehyde in PBS. Cleavage of the substrate by a proteinase results in unblocking of quenched fluorescence and an increase in intensity of fluorescence. Some of the sections were incubated with the potent zinc chelator 1,10-*O*-phenantroline (1 mM in DMSO; Molecular Probes), the MMP inhibitor *N*-[(2*R*)-2-(hydroxamidocarbonylmethyl)-4-methylpentanoyl]-L-tryptophan methylamide (final concentration, 50 μg/ml in 5% DMSO; Chemicon), or DMSO (5%; Sigma).

The optical density of the fluorescent signal was measured by NIH Image 1.62 (arbitrary units) in granular and molecular layers from control and kainate-treated brains ($n = 5$). Data were analyzed by Microsoft (Redmond, WA) Excel.

MMP isolation. Brains were rapidly removed, and cerebral cortex and hippocampus were dissected on a cold plate. By cutting along the rhinal fissure, cortex was divided into limbic cortex and neocortex. The complete sets of samples (from control and treated animals) were always processed, analyzed, and stored under the same conditions to avoid possible problems with autoactivation of MMPs. The dissected brain structures were processed separately. The extraction of MMPs from brain tissue followed the procedure by Weeks et al. (1976) originally developed to extract MMPs from rat uterus. Tissue samples were weighed and then homogenized in a buffer containing 10 mM $CaCl_2$ and 0.25% Triton X-100 in water (20 μl of buffer/1 mg of wet tissue); 0.75 ml of homogenates was centrifuged at $6000 \times g$ for 30 min. The entire supernatant containing soluble proteins was quantitatively recovered. The proteins from the supernatant were precipitated in 60% ethanol for 1 min at 4°C and than centrifuged at $15{,}000 \times g$ for 5 min. The precipitate was solubilized in 200 μl of sample buffer containing 2% SDS for 15 min at 37°C.

The pellet (Triton X-100-insoluble) was resuspended in a buffer containing 50 mM Tris, pH, 7.4, and 0.1 M $CaCl_2$ in water, heated for 15 min at 60°C, and then centrifuged at $10{,}000 \times g$ for 30 min at 4°C. This treatment results in releasing ECM-bound MMPs into the solution. The final pellet was free from MMP activities, as evaluated by gel zymography, which confirmed the completeness of the extraction. The final supernatant was considered a Triton X-100-insoluble fraction. After centrifugation, the entire supernatant was quantitatively recovered. The proteins from the supernatant were precipitated and finally solubilized in 200 μl of SDS sample buffer. Five microliters of the Triton X-100-soluble fraction (i.e., 1/40 of this fraction) containing 15 μg of total proteins and 30 μl of the Triton X-100-insoluble fraction (1/7 of this fraction) containing <0.15 μg of total proteins gave the MMPs bands of similar intensity when analyzed by gel zymography. Samples were equalized on the basis of the direct protein concentration measurements using the Bradford method as well as densitometry of protein bands after Coomassie blue G-250 or silver staining.

To characterize further the main form of MMP-2 detected in brain extracts, we incubated crude extracts of MMPs with the organomercurial compound *p*-aminophenylmercuric acetate (APMA; Sigma; 1 mM) at 37°C for 6 and 24 hr. APMA is known for its ability to catalyze the autocleavage of the proenzyme to active forms of lower molecular weight. After incubation, the extracts were mixed with sample buffer and subjected to gel zymography.

Gel zymography. The samples prepared from two fractions (Triton X-100-soluble and -insoluble) together with molecular weight standards (Sigma) or recombinant mouse proMMP-9 (5 ng/lane; Calbiochem, La Jolla, CA) and human proMMP-2 (5 ng/lane; R & D Systems, Minneapolis, MN) were subjected to electrophoresis using a Protean II system (Bio-Rad, Hercules, CA), in SDS-PAGE Tris-glycine 7.5% acrylamide gels containing 0.5% gelatin (Merck) under nondenaturating, nonreducing conditions. Gels were washed twice for 15 min in 2.5% Triton X-100 to remove SDS and incubated for 2 d in 50 mM Tris, pH 7.5, 10 mM $CaCl_2$, 1 μM $ZnCl_2$, 1% Triton X-100, and 0.02% sodium azide at 37°C. Gels were then stained with 0.1% Coomassie blue G-250 for 3 hr in 40% 2-propanol and destained with a solution containing 5% acetic acid until clear bands of gelatinolysis appeared on a dark background. Wet zymograms were digitized using a scanner (AGFA). To confirm that detected activities were zinc-dependent gelatinases, some zymogram gels were incubated with 1 mM 1,10-*O*-phenantroline (Merck), a broad-spectrum inhibitor of metalloproteinases. In parallel, equal volumes of the same samples were subjected to SDS-PAGE, and gels were stained with Coomassie blue or silver to verify that the protein content was equivalent across samples.

Immunoprecipitation. Tissue samples homogenized in lysis buffer (New England Biolabs; 20 μl of buffer per 1 mg of wet tissue) were centrifuged at 15,000 × *g* for 10 min at 4°C. Anti MMP-9 and anti-MMP-9 antibodies (1:500; Torrey Pines Biolabs) were added to 0.5 ml of supernatants and incubated for 24 hr at 4°C. The immunocomplexes were separated by incubating with 50 μl of protein A-Sepharose (Amersham Biosciences; 50% in TBS) for 4 hr at 4°C followed by centrifugation at 15,000 × *g* for 5 min at 4°C. The pellets were mixed with sample buffer and processed for zymography.

Western blot detection of MMP-9. Tissue extracts (Triton X-100-insoluble fraction) used for gel zymography were also used in parallel for Western blot analyses, except the samples were boiled and reduced with 1% β-mercaptoethanol. Samples and molecular weight standards (Sigma) were electrophoresed in SDS-PAGE acrylamide gels, transferred onto nitrocellulose membranes (Amersham Biosciences), and incubated for 24 hr in PBS, 5% nonfat milk, and 0.1% Tween 20 at 4°C. Membranes were then incubated for 2 hr at room temperature with anti-MMP-9 polyclonal antibody Ab.1 (Torrey Pines Biolabs; 1:2000 dilution), washed in PBS and 0.2% Tween 20, incubated for 1 hr at room temperature with HRP-conjugated anti-mouse antibody (Amersham Biosciences; 1:10,000), and revealed using the ECLplus chemiluminescent kit (Amersham Biosciences) following the manufacturer's instructions. Image digitalization was performed as described above.

Western blot detection of human recombinant MMP-9. Latent and active forms of human MMP-9 (0.1 μg; from R&D Systems and Calbiochem, respectively) were mixed with sample buffer, denatured, electrophoresed, blotted, and detected as described above.

Isolation of hippocampal molecular layer and MMP-9 analysis. Control and kainate-treated brains (24 hr) were frozen on dry ice and cryocut into 60 μm coronal sections. The upper molecular layer of dentate gyrus (DG) was dissected under the microscope using the needle tip. The tissue from two control and two treated (kainate, 24 hr) animals was pooled and collected in lysis buffer and then subjected to immunoprecipitation with anti-MMP-9 Ab.1.

Quantitative competitive reverse transcription (RT)-PCR analysis of the MMP mRNA levels. The hippocampi from control and kainate-treated (24 hr) rats were cut into 1.0-mm-thick slices on ice-cold agar plates. The dentate gyrus was then dissected out under a stereoscopic microscope. Total cellular RNA was isolated using Trizol (Invitrogen, San Diego, CA). One microgram of total cellular RNA was reverse-transcribed with random primers (Invitrogen) using Expand reverse transcriptase (Roche, Nutley, NJ). PCR was performed under standard conditions using *Taq* DNA polymerase (Qiagen, Hilden, Germany) and primers. Forward (5′-3′) and reverse (5′-3′) primers, respectively, were TCCTTCCTGGGTATGGAATC and ACTCATCGTACTCCTGCTTG for β-actin, CTATTCTGTCAGCACTTTGG and CAGACTTTGGTTCTCCAACTT for MMP-2, and AAATGTGGGTGTACACAGGC and TTCACCCGGTTGTGGAAACT for MMP-9. Amplified product lengths for β-actin, MMP-2, and MMP-9 were 300, 309, and 309 bp, respectively. Cycling conditions for β-actin gene and MMP-2 cDNAs were identical: 35 cycles of 95°C for 30 sec, 57°C for 30 sec, and 72°C for 120 sec and then holding at 4°C. Cycling conditions for amplification of MMP-9 were similar, with modification of the annealing step performed at 62°C for 30 sec. Ten microliters of the amplified product were then separated through 2% agarose gels containing 20 μg/ml ethidium bromide in Tris borate-EDTA buffer. Gels were visualized on a UV transilluminator, and digital images were taken using Scion Image PC.

Dentate gyrus MMP-2 and MMP-9 mRNAs levels were measured using methods established by Wells et al. (1996). Equal volumes of cDNA and threefold serial dilutions of the standard multicompetitor DNA were added to PCR. Multicompetitor DNA was an amplified product of a multicompetitor fragment of pQR2 (kindly provided by British Biotech). PCR was performed as described above. Ten microliters of the amplified product were then separated through 2% agarose gels containing 20 μg/ml ethidium bromide in 0.5× Tris borate-EDTA buffer. Gels were scanned on a Molecular Imager FX (Bio-Rad). Image analysis was performed on the scanned negative images of agarose gels using Quantity One, version 4.1.0 (Bio-Rad). Because longer DNA sequences incorporate proportionally more ethidium bromide molecules than shorter sequences, the pixel density of the shorter amplified product was normalized by multiplying it by the ratio of lengths in base pairs of the longer amplified product to the shorter amplified product. The log of the ratio of the normalized amplified product densities was plotted against the log of the concentration of the deletion standard RNA using Microsoft Excel 2000. The point at which the intensities of the two amplified products were equal (ratio = 1; log 1 = 0) defined the initial amount of MMP-2, MMP-9, or β-actin gene cDNA obtained from mRNA isolated from tissue samples.

Cultures of hippocampal neurons. Culture conditions were based on the system used by Blondel et al. (2000). Briefly, hippocampi were dissected from embryonic day 18 rat embryos (Taconic Farms, Germantown, NY). The tissue was digested with papain. After counting, the cells were plated on poly-L-ornithine (Sigma)-coated glass coverslips at a density of 200,000 cells per well in a 24 well plate (Costar, Cambridge, MA) and cultured for 2 weeks in modified minimal essential medium containing 5% horse serum and 1% bovine serum (Invitrogen). Cultures were fixed with 4% paraformaldehyde in PBS, washed, and co-immunostained as described above with anti-MMP-9 Ab.1 and a monoclonal antibody against neuron-specific type III β-tubulin; (TUJ1; 1:500; Covance).

RESULTS

MMP-9 and MMP-2 are differentially distributed in the adult rat brain

Considering that past results have been inconsistent with respect to the cellular localization of MMPs in the brain (Del-Bigio and Jacque, 1995; Backstrom et al., 1996; Gottschall and Deb, 1996; Lim et al., 1996; Romanic et al., 1998), we first investigated the tissue distribution of MMPs within the rat forebrain by means of *in situ* hybridization and immunocytochemistry. Coronal sections of 2-month old rat brains were analyzed at the level of the dorsal hippocampus (Fig. 1*A*). MMP-9 mRNA was preferentially localized within the hippocampus to the pyramidal cell layers of cornu ammonis 1 (CA1) and CA3 and the granule cell layer of the DG (Fig. 1*B*). Other structures within the limbic system, such as piriform cortex and amygdala, as well as nonlimbic regions (e.g., neocortex) were also found to express an MMP-9 message (results not shown). In contrast, MMP-2 mRNA was rather uniformly distributed, especially within the brain gray matter, and was generally expressed at a lower level then MMP-9 (Fig. 1*C*). We did not observe enrichment of MMP-2 message in the CA fields or the DG.

Immunohistochemical staining with selective polyclonal antibodies raised against the catalytic domains of rat recombinant MMP-9 and MMP-2 was used to study the protein distribution of the MMPs. The overall pattern of the MMP protein distribution paralleled that of the MMP mRNA expression as revealed by *in situ* hybridization (Fig. 1). Generally, MMP-9 protein was primarily expressed within neuronal subfields as well as diffusely especially in the lacunosum molecular layer, whereas MMP-2 protein was more diffusely distributed and expressed at a lower level.

The distribution pattern of MMPs in the hippocampus suggests that MMP-9 is primarily but not exclusively expressed by neurons, whereas MMP-2 originates primarily from glial cells. To

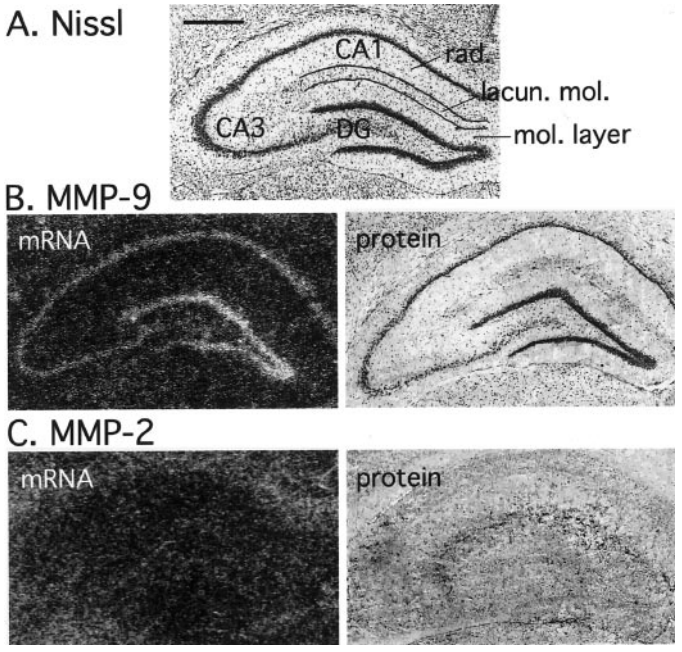

Figure 1. Tissue distribution of MMP-9 and MMP-2 in adult rat brain. Sections of dorsal hippocampus demonstrating the distribution of MMP-9 and MMP-2 mRNA and protein are shown. *A*, Nissl staining of a hippocampal coronal section. *mol. layer*, Molecular layer; *lacun. mol.*, lacunosum molecular layer; *rad.*, radiatum layer. Scale bar, 1 mm. *B*, Tissue distribution of MMP-9 mRNA (*in situ* hybridization; *left image*) and protein (immunohistochemistry; *right image*). MMP-9 mRNA is enriched in neuronal fields of the hippocampus. The *right image* shows enrichment of MMP-9 protein in neuronal bodies of the dentate gyrus and the CA subfields. Diffuse MMP-9 protein staining, especially in the lacunosum molecular layer, can also be discerned. *C*, Tissue distribution of MMP-2 mRNA (*left image*) and protein (*right image*). In contrast to MMP-9, MMP-2 mRNA and protein are diffusely distributed over the entire hippocampus.

better illustrate this finding, we immunostained brain sections with anti-MMPs antibodies and doubled labeled cells with either NeuN or the astrocytic marker GFAP. As illustrated in Figure 2*A*, MMP-9 antibody was colocalized with NeuN-positive granule neurons within the DG. In addition, a fraction of GFAP-positive astrocytes was also MMP-9-positive (Fig. 2*B*, *arrows*). At the subcellular level, MMP-9 was detected primarily in the perinuclear region. However, with aid of the neuronal maker MAP-2, we were able to demonstrate that MMP-9 was also localized within neuronal dendrites. The dendritic localization of MMP-9 was most clearly seen in neocortex, as shown in Figure 2*C*. In contrast to MMP-9, MMP-2 antibody strongly recognized astrocytes, although faint staining of DG granule neurons could also be detected (Fig. 2*D*).

To investigate further subcellular localization of MMP-9, we co-immunostained dissociated hippocampal neurons in culture with anti-MMP-9 antibody Ab.1 and anti-TUJ1 antibody (Fig. 3). Although dissociated neurons did not show clear neuritic expression of the enzyme at low magnification (*top images*), when the cells were analyzed at high magnification, MMP-9 protein was localized clearly in TUJ1-positive neuronal processes (*bottom images*).

MMP-9 is enzymatically active in the adult rat brain

Results presented above suggest that MMPs are functional in the adult brain. To test this directly, we analyzed the enzymatic

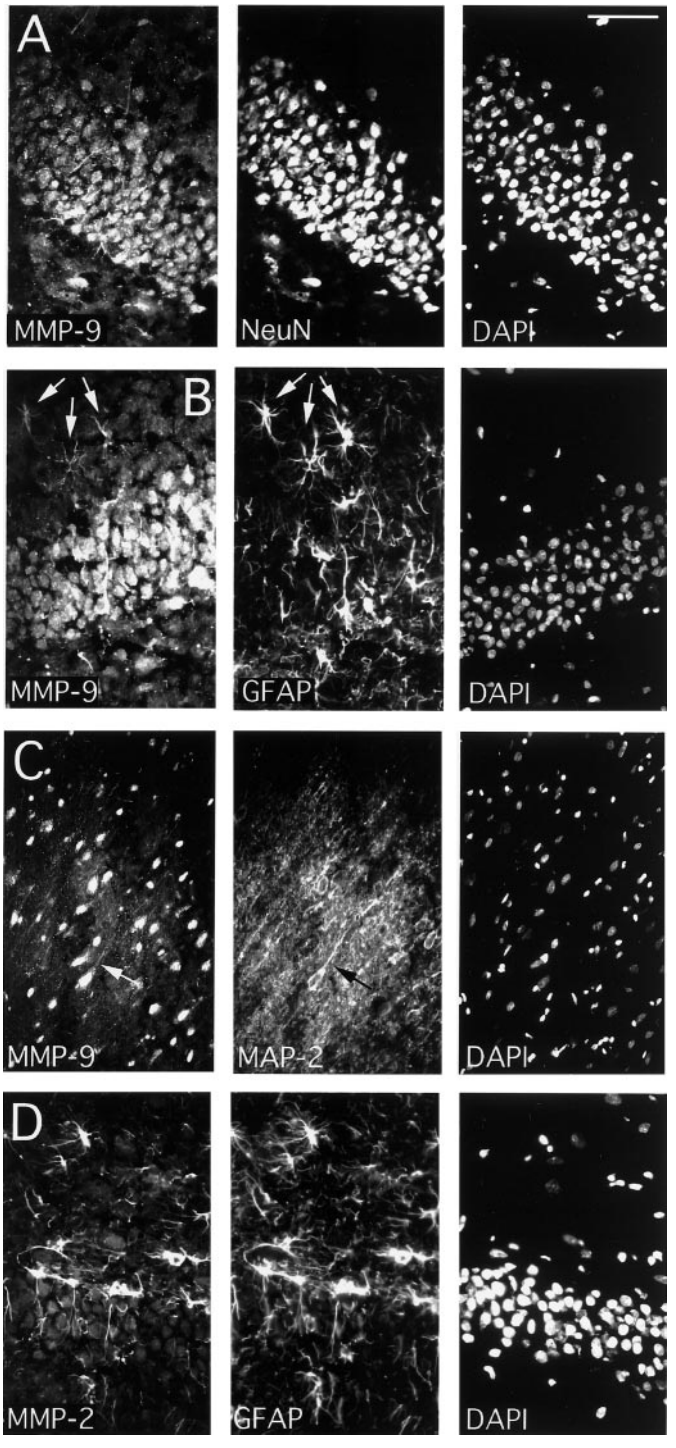

Figure 2. Cellular localization of MMP-9 and MMP-2 protein in adult rat brain. Colocalization of MMPs with cell type-specific markers is shown. *A*, DG staining with MMP-9 (*left image*) and the neuronal maker NeuN (*middle image*). Note NeuN-positive granule neurons that are MMP-9 positive. Cell nuclei are labeled with DAPI (*right image*). *B*, DG staining with MMP-9 (*left image*) and the astrocyte marker GFAP (*middle image*). *Arrows* indicate astrocytes that express MMP-9 protein. Cell nuclei are labeled with DAPI (*right image*). *C*, Neocortex staining with MMP-9 (*left image*) and the dendritic marker MAP-2 (*middle image*). *Arrows* indicate MMP-9-positive dendrites. Cell nuclei are labeled with DAPI (*right image*). *D*, DG staining with MMP-2 (*left image*) and GFAP (*middle image*). Note GFAP-expressing astrocytes that are MMP-2 positive. Cell nuclei are labeled with DAPI (*right image*). Scale bar, 50 μm.

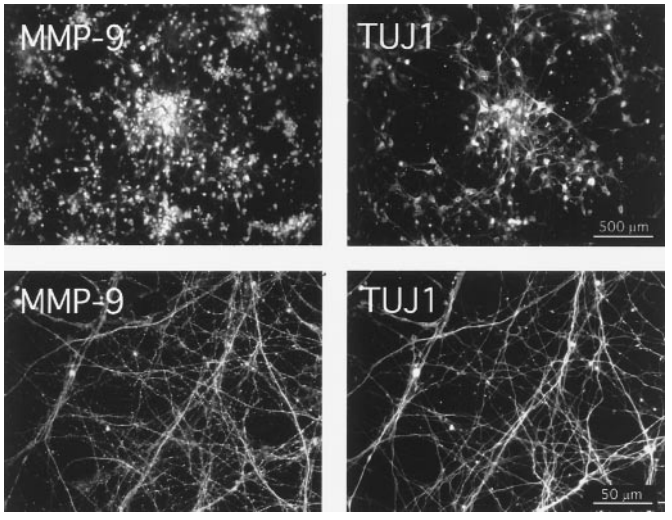

Figure 3. MMP-9 is localized in neuronal processes of cultured hippocampal neurons. Co-immunostaining of dissociated hippocampal neurons in culture with anti-MMP-9 antibody Ab.1 and anti-TUJ1 antibody is shown. Although dissociated neurons did not show clear neuritic expression of the enzyme at low magnification (*top images*; scale bar, 500 μm), when the cells were analyzed at high magnification, MMP-9 protein was localized clearly in TUJ1-positive neuronal processes (*bottom images*; scale bar, 50 μm).

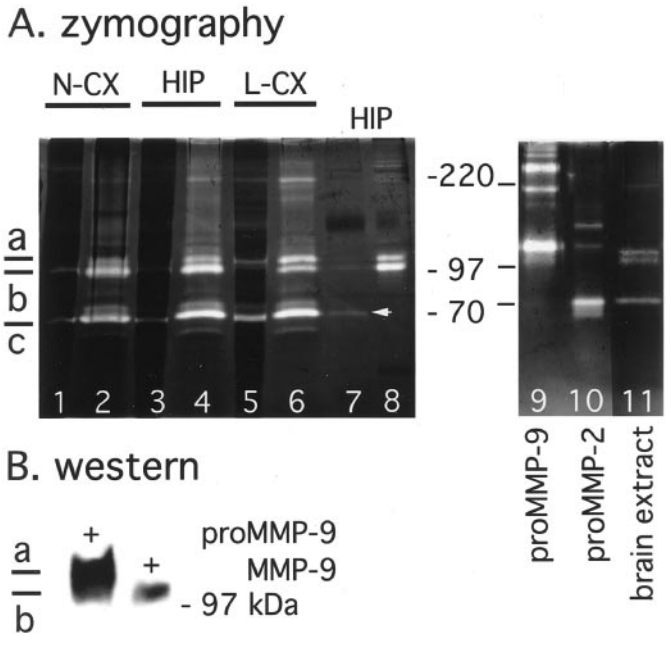

Figure 4. Characterization of MMP activities from rat brain. *A*, Gel zymography of brain extracts (see details in Materials and Methods). *Left image*, Triton X-100-soluble (*lanes 1, 3, 5*) and -insoluble (*lanes 2, 4, 6*) fractions from neocortex (*N-CX*), hippocampus (*HIP*), and limbic cortex (*L-CX*) show a similar molecular pattern of enzymatic activities of MMPs. Two main activities at ~97 kDa (*bands a, b*) and one at 70 kDa (*band c*) can be detected. Note the enrichment of MMPs in the Triton X-100-insoluble fraction. Immunoprecipitation with the selective anti-MMP-2 (*lane 7*) or anti-MMP-9 (*lane 8*) antibody confirms that the 97 kDa doublet consists of latent (*band a*) and active (*band b*) forms of MMP-9 (*lane 8*), whereas the 70 kDa activity is MMP-2 (*line 7*). *Right image*, One hundred five kilodalton recombinant mouse proMMP-9 (latent MMP-9; *lane 9*) and 70 kDa recombinant human proMMP-2 (latent MMP-2; *lane 10*) were co-electrophoresed with MMPs extracted from rat hippocampus (*lane 11*). Mouse MMP-9 migrates slightly above extracted rat 97 kDa gelatinase, whereas MMP-2 migrates directly at the level of extracted 70 kDa gelatinase. The discrepancy in MMP-9 migration is related to differences in both protein size and level of glycosylation. *B*, Western blot of latent (*proMMP-9*) and active forms of human recombinant MMP-9 detected with the anti-rat-MMP-9 antibody. Note that the anti-rat-MMP-9 antibody cross-reacts with human MMP-9.

activities of brain MMPs by gel zymography with gelatin as a substrate. Protein extracts from various brain regions were divided into either Triton X-100-soluble or -insoluble fractions. The latter is enriched in ECM proteins. Although MMPs may exist in various forms differing in molecular weight and activity, these enzymes primary exist in either a latent (proenzyme) or active form. The latent form is ~10 kDa larger then the active form because of the propeptide sequence, which is cleaved off on activation. In brain extracts, we were able to detect three main gelatinolytic activities. First, a double band at >97 kDa, presumably reflecting the latent and active forms of MMP-9 as estimated on the basis of known molecular weight for the enzyme (Fig. 4*A*, *left image*, *bands a, b*). Extracted MMP-9 migrated slightly below recombinant mouse proMMP-9 (105 kDa; Fig. 4*A*, *right image*). The discrepancy in MMP-9 migration is related to the fact that MMP-9 from various species differs in protein size as well as the level of glycosylation. Second, a predominant band at 70 kDa presumably reflects MMP-2 (Fig. 4*A*, *left image*, *band c*). The 70 kDa form may be classified as the latent form (proenzyme), because it gave rise to lower molecular weight forms on autocleavage catalyzed by the organomercurial compound APMA (see Materials and Methods; data not shown). The identity of this band was further confirmed by showing co-migration of extracted MMP-2 with recombinant human pro-MMP-2 (Fig. 4*A*, *right image*). Finally, we detected other activities at ~220 kDa. The MMPs were present in both the Triton X-100-soluble (Fig. 4*A*, *lanes 1, 3, 5*) and -insoluble (Fig. 4*A*, *lanes 2, 4, 6*) fractions, however, at different levels. Because the total protein concentration in Triton X-100-soluble fraction was ~100 times higher than in the fraction extracted from Triton X-100-insoluble pellet, we assumed that MMPs were enriched in the later fraction. Extracts from neocortex, limbic cortex, and hippocampus did not show significant differences in the pattern of MMP activities (Fig. 4*A*).

Because contradictory results have been published on the immunolocalization of MMPs in nervous tissue, we controlled our antibodies very thoroughly. Specificity of the antibodies used for immunostaining were verified by immunoprecipitation of respective MMPs from hippocampal extracts with zymography as a read-out. As shown in Figure 4*A*, *lane 8*, anti-MMP-9 antibody precipitated two main gelatinolytic activities at ~97 kDa (*bands a, b*) as well as bands at ~220 kDa, presumably either MMP-9 dimer or a complex with other proteins (Woessner, 1995). Similar high molecular weight forms were seen when recombinant MMP-9 was subjected to analysis (Fig. 4*A*, *lane 9*). The anti-MMP-2 antibody recognized the activity of the 70 kDa band (*band c*), however, at much lower efficiency then the MMP-9 antibody did with MMP-9 (Fig. 4*A*, *lane 7*). The anti-MMP-2 antibody recognized weak activity at ~97 kDa. Similar high molecular weight forms were seen when recombinant preMMP-2 was analyzed (Fig. 4*A*, *lane 10*). In addition, anti-rat MMP-9 antibody recognized human recombinant latent and active MMP-9 on Western blotting (Fig. 4*B*). Moreover, incubation of the anti-MMP-9 antibody with the rat recombinant MMP-9 (against which the antibody was raised) before immunostaining significantly decreased the intensity of staining in neuronal cell bodies and attenuated the diffuse staining seen within the hip-

pocampus (see Materials and Methods; data not shown). In addition, immunostaining with a different anti-MMP-9 antibody, Ab.2, was highly compatible with anti-MMP-9 Ab.1 staining (see Materials and Methods; data not shown).

Kainate induces selective neurodegeneration in adult rat brain

Intraperitoneal delivery of kainate produces substantial enhancement of synaptic activity resulting in a characteristic pattern of limbic seizures. These effects persist several hours after drug administration. This seizure activity can result in the death of pyramidal neurons in the CA regions of the hippocampus as well as cells in limbic cortex and amygdala 24–72 hr after drug treatment (Pollard et al., 1994). The degree and localization of neuronal loss varies between animals as well as animal strains (Sperk, 1994). In our hands, Wistar rats with seizures developed CA1 degeneration in 50% of the cases, whereas limbic cortex and amygdala were lesioned in 80% of the animals. Typical histopathological changes after the drug application, visualized by Nissl staining, are shown in Figure 6*E–H*.

Kainate differentially regulates MMP-9 and MMP-2 gene expression and enzymatic activity

As described above, MMP-9 is present in neurons within the limbic system and neocortex. To test responsiveness of the MMPs to neuronal activity, we used a model of kainate-induced limbic system activation and remodeling. In hippocampus, latent MMP-9 activity increased as early as 2 hr after kainate treatment, reaching a peak at 6 hr (Fig. 5*A*, *band a*). At 24 hr, latent MMP-9 activity decreased but still remained above control levels. Decrease of latent MMP-9 after 24 hr was accompanied by upregulation of the active form of the enzyme (Fig. 5*A*, *band b*). The increase in the 220 kDa MMP-9 form was also observed after kainate treatment. The kinetics of change in MMP-9 activity was similar in either Triton X-100-soluble or -insoluble fractions (Fig. 5*A*). In contrast to MMP-9, the activity of MMP-2 did not undergo elevation at either 6 or 24 hr after kainate administration (Fig. 5*A*, *band c*).

To further confirm that the observed changes in the 97 kDa gelatinolytic activities reflected MMP-9 activation, we performed immunoprecipitation with the anti-MMP-9 antibody on postkainate hippocampal protein extracts, followed by zymography (Fig. 5*B*). The latent form of MMP-9 was upregulated 6 hr after kainate treatment, whereas the increase in the active form was not detected until 24 hr after treatment. In addition, Western blotting of MMP-9 in the Triton X-100-insoluble fraction revealed a clear upregulation of the latent form as early as after 6 hr after treatment, with both forms being upregulated after 24 hr (Fig. 5*C*).

We also investigated kainate-induced changes in the expression of both MMP-2 and MMP-9 in brain sections using *in situ* hybridization and immunocytochemistry. Kainate treatment induced upregulation of MMP-9 mRNA after 24 hr in the DG and neocortex (Fig. 6). In contrast, the MMP-9 message was downregulated in piriform cortex and amygdala. This downregulation of MMP-9 message was positively correlated with neurodegeneration in these two brain regions (Fig. 6, *Nissl*). Interestingly, MMP-9 mRNA was present predominantly in the granule cell layer in control DG, whereas after kainate treatment the message was upregulated in the granular layer, the site of neuronal cell bodies, and the molecular layer, which contains neuronal dendrites (Fig. 7). We could detect this redistribution pattern as early as 12 hr after kainate administration in 2 of 4 brains tested.

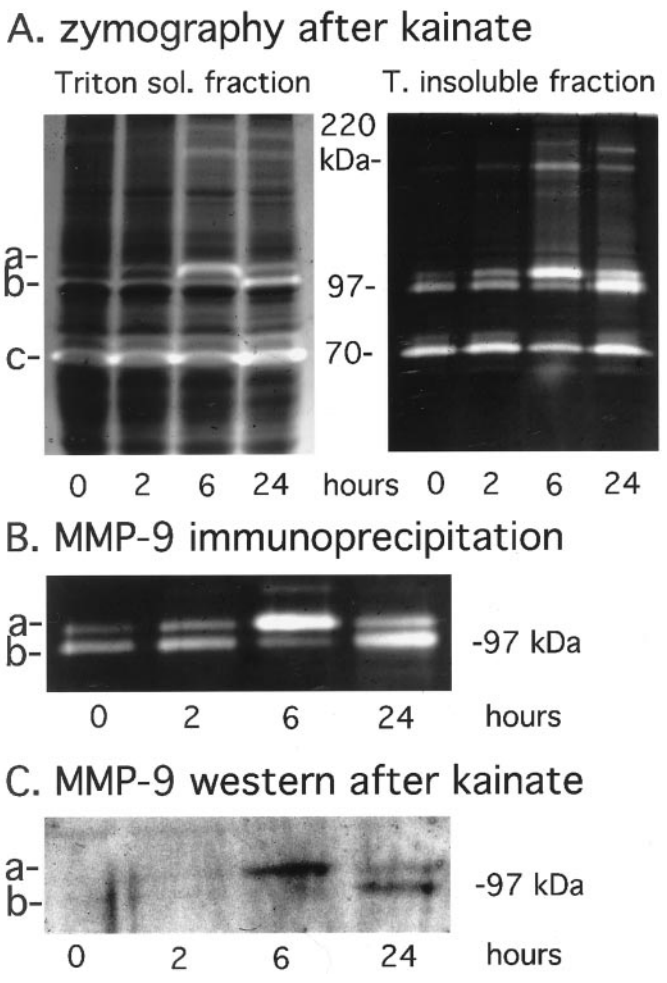

Figure 5. Kainate upregulates MMP-9 protein and induces its enzymatic activation. *A*, Representative sets of zymograms of either Triton X-100-soluble or -insoluble fractions from rat hippocampi after kainate treatment. Activities of latent (*band a*) and active (*band b*) MMP-9 are upregulated after 6 and 24 hr, respectively. The activity of MMP-2 remains unchanged (*band c*). *B*, Zymographic analysis of MMP-9 immunoprecipitated with the selective anti-MMP-9 antibody (Ab.1) from hippocampal protein extracts obtained from kainate-treated rats (from the same animals as analyzed in *A*). Activities of latent (*band a*) and active (*band b*) MMP-9 are upregulated after 6 and 24 hr, respectively. *C*, MMP-9 Western blot analysis of Triton X-100-insoluble fractions from hippocampal protein extracts after kainate treatment (from the same animals analyzed in *A*). Samples from Triton X-100-insoluble fractions at different time points (0, 2, 6, and 24 hr) were subjected to Western blotting with the anti-MMP-9 antibody. Latent (*band a*) and active (*band b*) forms of MMP-9 are upregulated after 6 and 24 hr, respectively.

Twenty-four and 72 hr after kainate treatment, we detected MMP-9 upregulation and redistribution in 6 of 11 and 2 of 3 brains, respectively. MMP-2 mRNA was found to be clearly downregulated in degenerated brain regions at 24 and 72 hr after kainate administration (Fig. 6).

We used quantitative RT-PCR to further confirm, that MMP-9 mRNA was upregulated in the DG after kainate treatment (Fig. 8). This approach is based on competition between target and competitor DNA that occurs during PCR (Wells et al., 1996). To reduce differences in target and competitor amplification kinetics, we used the fragment of the pQR2 gene as a competitor. This fragment has a similar structure to that of the target genes under investigation (i.e., MMP-9, MMP-2, and $\beta-$actin). To test for

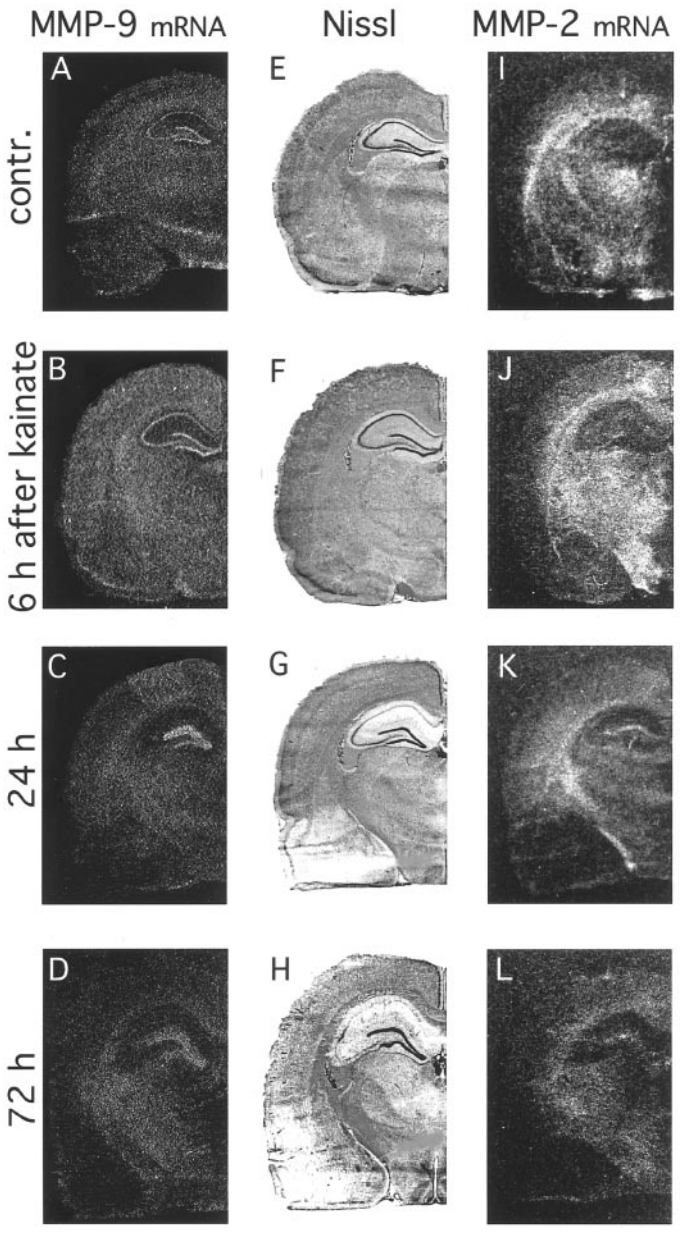

Figure 6. *In situ* hybridization detection of MMP-9 and MMP-2 mRNAs after kainate treatment. Rat brain sections subjected to either Nissl staining (*middle images*) or *in situ* hybridization with MMP-9 (*left images*) or MMP-2 (*right images*) radiolabeled cDNA probes. Sections were made from either control (*contr.*) animals (*A, E, I*) or kainate-treated animals at 6, 24, and 72 hr after drug administration (*B–L*). Kainate treatment causes neurodegeneration and significant tissue deterioration after 24 and 72 hr in piriform cortex and amygdala as visualized by the decrease in intensity of the Nissl staining (*G, H*). Kainate treatment results in upregulation of MMP-9 mRNA in DG (*B–D*) and downregulation in degenerating limbic areas (*C, D*). MMP-2 mRNA was downregulated in lesioned limbic areas (*K, L*).

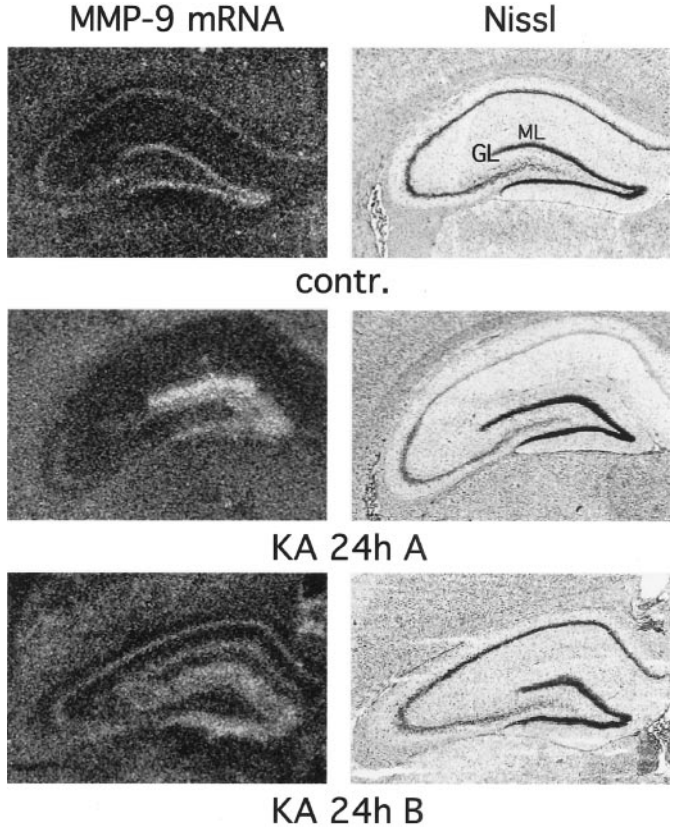

Figure 7. Kainate induces redistribution of MMP-9 message in the dentate gyrus. *In situ* hybridization detection of MMP-9 mRNA in rat hippocampi, control (*contr., top images*) and 24 hr after kainate-induced seizures (two representative brains, *A, B*) is shown. Rat brain sections were subjected to either *in situ* hybridization with the MMP-9-radiolabeled probe (*left images*) or Nissl staining (*right images*). Note enhancement and relocation of MMP-9 mRNA from the granular layer (*GL*) to the molecular layer (*ML*) of the dentate gyrus.

variations in mRNA levels between samples, β-actin gene expression was used as an internal standard for each sample. The mean normalized MMP-9 expression level in the DG 24 hr after kainate treatment reached 0.55 (SD, 0.04) of the abundance of β-actin mRNA, whereas in control DG, the amount of MMP-9 mRNA was equal to 0.0002 (SD, 0.0001) of β-actin mRNA. In contrast, MMP-2 mRNA abundance values in the same samples were 0.00065 (SD, 0.002) in control DG and 0.00056 (SD, 0.001) 24 hr after kainate.

We also investigated whether there was a correlation between the induction of MMP-9 mRNA in the molecular layer of the DG and degeneration in the CA1 subfield and the piriform cortex and amygdala, which functionally connect to the DG. MMP-9 upregulation in the DG was detected in 2 of 5 brains with CA1 degeneration. However, in 4 of 6 brains with a morphologically intact CA1 field, MMP-9 message was also upregulated in the DG. In 9 of 11 animals that displayed long-lasting limbic seizures, lesions in the piriform cortex and amygdala were observed 24 hr after kainate application. Six of 9 of these showed upregulation of MMP-9 mRNA within dentate molecular layer. The two brains from animals without piriform cortex lesions displayed no changes in MMP-9 mRNA redistribution. Although most animals with piriform cortex lesions responded with MMP-9 mRNA redistribution, other factors in addition to cortical lesions, such as intensity or a unique pattern of seizures, may be responsible for MMP-9 mRNA relocation.

After kainate treatment, the expression pattern of MMP-9 protein shared partial similarities with changes described for MMP-9 mRNA (Fig. 9). A moderate increase in MMP-9 immunostaining in the neuronal cell bodies of the hippocampus was seen at 6 hr after kainate application. We did not notice any clear upregulation of MMP-9 immunostaining in primary dendrites at

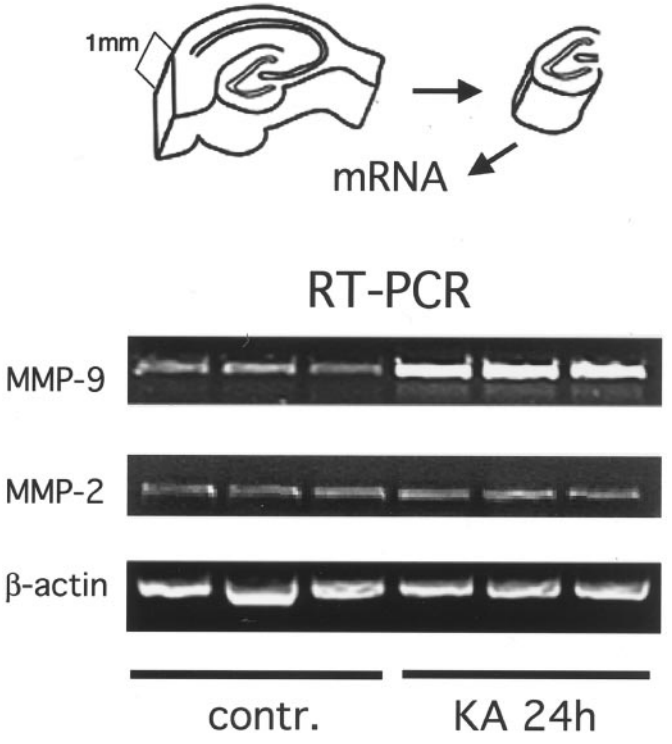

Figure 8. Increase of MMP-9 mRNA in the DG detected by RT-PCR after kainate treatment. The DG was removed from 1-mm-thick hippocampal slices and subjected to total cellular RNA extraction. RT-PCR analysis demonstrated that DG MMP-9 mRNA was upregulated 24 hr after kainate treatment. No changes were seen for MMP-2 and β-actin mRNAs. *contr.*, Control.

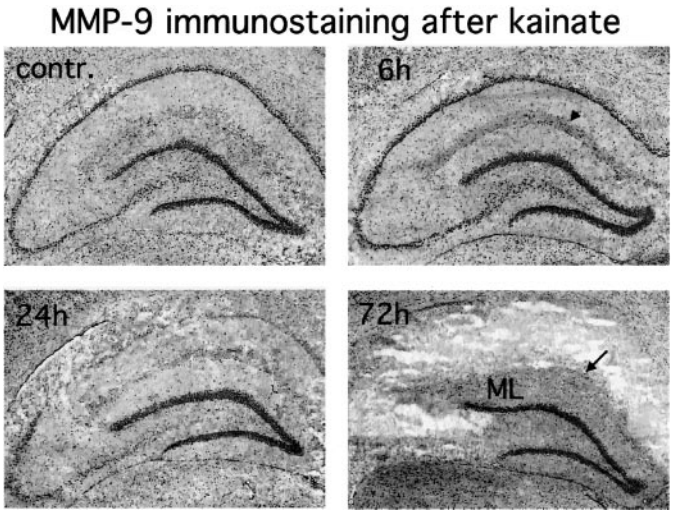

Figure 9. MMP-9 immunostaining in kainate-treated brains. Representative images show MMP-9 protein expression in hippocampus at different time points after kainate treatment. The *arrowhead* indicates enhancement of diffuse staining in the lacunosum molecular layer. The *arrow* indicates the border between the molecular layer (*ML*) of the DG and the lacunosum molecular layer of CA1. MMP-9 protein was upregulated in the granular layer 6 hr after the treatment. Seventy-two hours after kainate treatment, diffuse staining of MMP-9 was enhanced in the DG, whereas in the CA subfields, MMP-9 was downregulated. Note that kainate produced neurodegeneration resulting in partial deterioration of the hippocampus (CA3 and CA1 fields). *contr.*, Control.

any time after the seizures; however, in ~50% of the brains (n = 8 for the 6 hr time point; n = 5 for the 12 hr time point), we observed enhancement of diffuse staining in the lacunosum molecular layer (Fig. 9, *arrowhead*). After 72 hr, the MMP-9 protein staining within dentate molecular layer was enhanced in all of the brains tested [n = 4; Fig. 9, *arrow* indicates the border between the molecular layer (*ML*) of the dentate gyrus and CA1]. Co-immunostaining of MMP-9 together with astrocyte marker GFAP and neuronal marker NeuN, 24 hr after kainate application, confirmed that MMP-9 immunostaining was enhanced in DG neurons but not astrocytes (Fig. 10). Twenty-four and 72 hr after kainate treatment, MMP-9 immunostaining was attenuated within the damaged CA fields (Fig. 9). We did not notice any upregulation of MMP-2 immunostaining (data not shown).

Because the activity assay has proven to be the most sensitive mean for MMPs detection, we analyzed behavior of MMPs using *in situ* zymography. Brain sections were incubated with gelatin conjugated to quenched fluorescent dye. Cleavage of gelatin results in an increase of fluorescence. The pattern of gelatinase activity in hippocampus resembled MMP-9 localization (Fig. 11). Gelatinase activity was inhibited by the zinc chelator phenantroline and the inhibitor of MMPs (Fig. 11). Kainate treatment was found to upregulate gelatinase activity in the granular and molecular layers of the DG (Fig. 12*A*). NIH Image software was used to measure gelatinase activity within the granular and molecular layers. In the control sections, the mean optical density (expressed in arbitrary units) of the granular layer was 68 ± 5.7 (n = 5), whereas the mean optical density of the molecular layer was 25 ± 1.4. After kainate administration (24 hr time point), the mean optical density of the granular layer was 120 ± 15 (n = 5), whereas the mean optical density of the molecular layer was 46 ± 5. The differences between control and kainate-treated brains were statistically significant by t test ($p < 0.01$). Furthermore, by performing immunoprecipitation of MMP-9 (anti-MMP-9 Ab.1) from the isolated molecular layers (n = 2), combined with gel zymography, we confirmed that MMP-9 was upregulated in DG molecular layer by kainate treatment (Fig. 12*B*).

DISCUSSION

The major findings of our study could be summarized as follows: (1) MMP-9, but not MMP-2, is highly expressed by neurons in adult rat brain; MMP-9 protein is enriched in neuronal cell bodies and is present in dendrites; (2) kainate-driven enhancement in synaptic activity upregulates the level of MMP-9 protein as well as its enzymatic activation; (3) kainate produces an increase in MMP-9 mRNA and enzymatic activity in the DG, the area known to be undergoing structural remodeling; and (4) kainate administration produces a decrease in MMP-9 in areas undergoing neuronal cell loss. These findings, as well as their possible implications for understanding MMPs role in cellular physiology, are discussed below.

Distribution of MMP-9 and MMP-2 in adult rat brain

To assess the quality of the experimental tools used, we first characterized the MMP-9 antibody by demonstrating that (1) the antibody immunoprecipitated two gelatinolytic activities at ~97 kDa, the known molecular weight for MMP-9, but not 70 kDa MMP-2; (2) the antibody cross-reacted with human recombinant latent and active forms of MMP-9, as visualized by Western blotting; and (3) recombinant MMP-9 protein blocked MMP-9 immunostaining in brain sections. In contrast, anti MMP-2 antibody was less selective, because it cross-reacted weakly with MMP-9 in immunoprecipitation experiments.

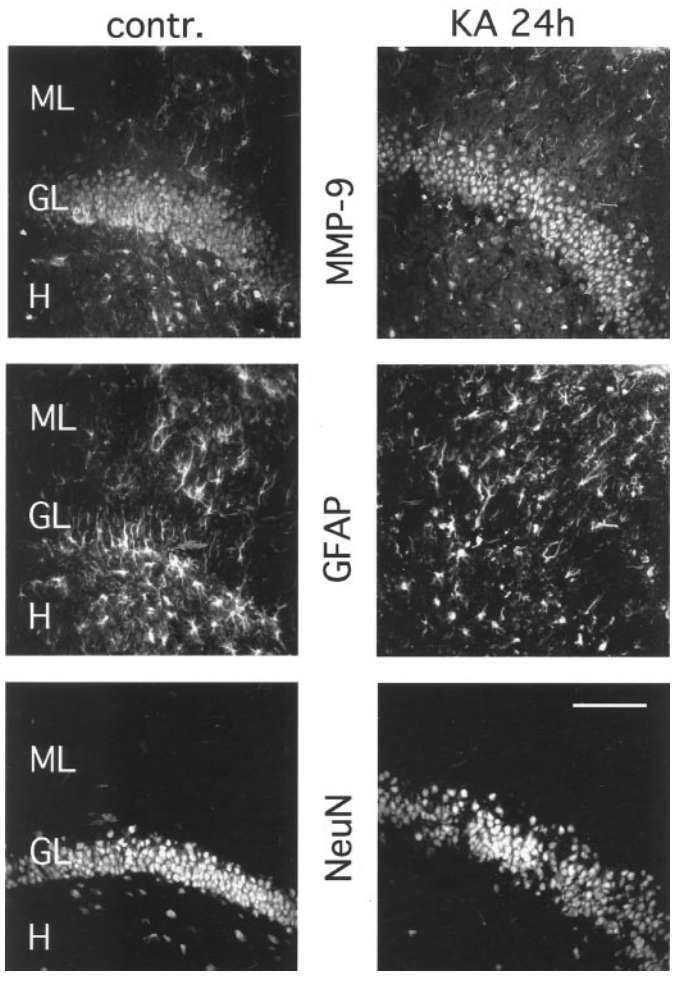

Figure 10. Cellular localization of MMP-9 protein in kainate-treated brains. Colocalization of MMP-9 protein with cell type-specific markers is shown. In control (*contr., left images*) and 24 hr after kainate application (*right images*), DG staining with MMP-9 (*top images*) and the astrocyte marker GFAP (*middle images*) is shown. Sections from the same animals were stained with the neuronal marker NeuN (*bottom images*). MMP-9 immunostaining was enhanced in the granular layer (*GL*) and molecular layer (*ML*). *H*, Hilus. Scale bar, 120 μm.

We focused our attention primarily on the hippocampus, a structure well characterized with respect to spatiotemporal expression of plasticity-related genes and that is known to undergo significant structural plasticity. By using both *in situ* hybridization and immunohistochemistry, we clearly demonstrated that under normal conditions MMP-9 but not MMP-2 was enriched in neuronal subfields within the hippocampus. Colocalization studies showed MMP-9 to be strongly expressed by neurons and to a lesser degree by glial cells, whereas MMP-2 was expressed predominantly by astrocytes. At the subcellular level, neuronal MMP-9 was highly enriched in the perinuclear compartment of neuronal cell bodies; however, we were also able to localize the protein within or near primary dendrites of cortical cells. Moreover, using an *in vitro* model of dissociated hippocampal neurons, we demonstrated clearly that MMP-9 protein was localized to neurites. However, we failed to show clear dendritic staining of MMP-9 in the DG, likely because of the high density of neuronal processes in the DG.

The close apposition of MMP-9 immunostaining with neuronal dendrites together with its diffuse staining pattern *in vivo* suggests

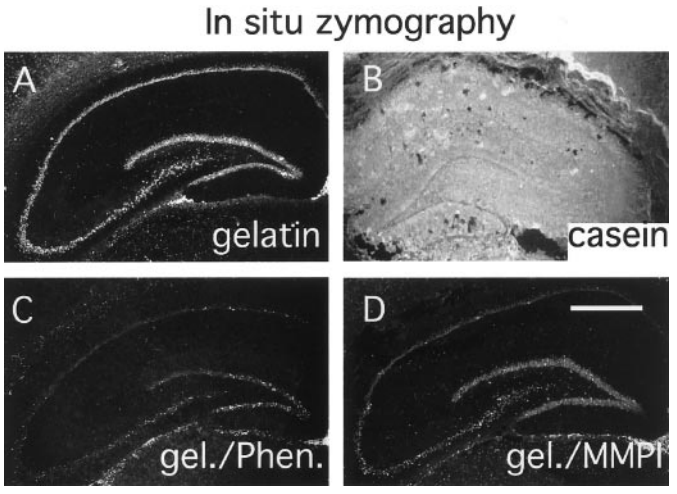

Figure 11. *In situ* zymography detects gelatinase activity in hippocampal sections. Brain sections were incubated with different fluorescent substrates: gelatin (gelatinase substrate; *A, C, D*) and casein (panproteinase substrate; *B*). Cleavage of the substrate by a proteinase results in unblocking of quenched fluorescence and an increase in fluorescence. Note that the pattern of gelatin cleavage resembles MMP-9 distribution (*A*). Gelatinase (*gel.*) activity is attenuated by the zinc chelator 1,10-*O*-phenantroline (*Phen., C*) and the synthetic MMP inhibitor (*MMPI, D*; see details in Materials and Methods). Scale bar, 1 mm.

that the enzyme may be located within dendritic ECM. This was further strengthened by the fractionation experiment. Although most of both MMP-2 and MMP-9 activities were present in the Triton X-100-soluble fraction containing primarily cytoplasmic and cell membrane proteins, MMPs were concentrated in the Triton X-100-insoluble fraction, which is enriched with ECM proteins. A unique feature of gelatinases (MMP-9 and MMP-2) in comparison with other MMPs is their ability to bind selectively to large structural proteins of ECM through the ECM-binding domain (Olson et al., 1998). The MMP activities present in the Triton X-100-soluble fraction may reflect newly synthesized proteins or a pool of membrane-bound MMPs (Yu and Stamenkovic, 2000).

Previous attempts to visualize MMP-9 protein within normal hippocampal neurons have not been successful, although the enzyme has been detected in both glia cells and pathological neurons (Backstrom and al., 1996; Lampert et al., 1998). Recently, neuronal expression of MMP-9 protein within the rat cerebellum has been reported (Vaillant et al., 1999). Interestingly, in the developing cerebellum, MMP-9 immunostaining was present in bodies as well as processes of Purkinje neurons, whereas in the adult cerebellum, MMP-9 immunostaining was primarily cytoplasmic. In contrast to our results, Vaillant et al. (1999) found that anti-MMP-2 antibody clearly stained cerebellar neurons as well as their dendrites but not glia cells. Other authors have detected MMP-2 protein at axonal growth cones (Zuo et al., 1998). The discrepancy between previous reports and the present data with regard to the localization of MMP-2 primarily to astroglia may be explained by the difference in antibodies used in these studies. Taken together, our and other authors data indicate that the MMPs are expressed by adult CNS neurons. The MMP expression level and cellular localization may be regulated according to the developmental or functional status of neurons, or both.

Regulation and mechanisms of MMP-9 expression in adult rat brain

In this report, we show that kainate treatment results in upregulation of MMP-9 mRNA, protein, and enzymatic activity with

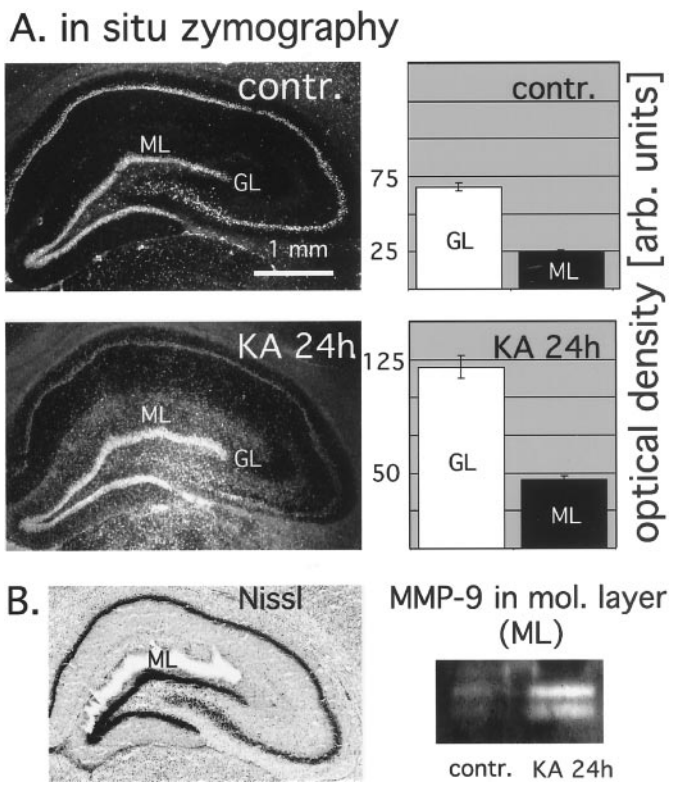

Figure 12. Kainate upregulates gelatinase activity in granular and molecular layers of the hippocampus. *A*, Brain sections from control (*contr.*) and kainate-treated (*KA*; after 24 hr) brains were analyzed by means of *in situ* zymography. The optical density of the granular layer (*GL*) and molecular layer (*ML*) were measured by NIH Image software (*graphs*). Note, that the kainate treatment enhances gelatinase activity in both granular and molecular layers of the hippocampus (differences between control and kainate-treated brains are statistically significant by *t* test; $p < 0.01$; $n = 5$; error bars represents SEM). *B*, Control and kainate-treated brains (24 hr; $n = 2$) were cryocut into 60 μm sections. The upper molecular layer (*mol. layer, ML*) of the DG was dissected from sections under the microscope, collected in lysis buffer, and subjected to immunoprecipitation with anti-MMP-9 Ab.1. *Left image*, Nissl-stained hippocampus from which the molecular layer was dissected. *Right image*, Upregulation of MMP-9 activity within the molecular layer after kainate treatment.

unique spatiotemporal characteristics. As we demonstrate by means of both zymography and Western blotting, MMP-9 latent protein was upregulated as early as 6 hr after seizures. This was followed by an increase in the active form of the enzyme 24 hr after kainate administration, indicating the enzymatic activation of MMP-9. Thus, although enhanced synaptic activity is able to induce MMP-9 protein accumulation at earlier times, additional factors seem to be required for MMP-9 to be converted to an active form during later times. Consistent with these findings is a recently published report demonstrating the rapid upregulation and late activation of MMP-9 after kainate-induced seizures (Zhang et al., 1998). These experiments suggest that synthesis of pro-MMP-9 and the enzyme activation are regulated independently. This is further supported by studies investigating MMPs and cortical injury in which latent MMP-9 was upregulated 3 hr after injury; however, this was not followed by enzymatic activation (Wang et al., 2000). Similarly, in Alzheimer's disease brains, latent MMP-9 has been reported to be elevated without any changes in the amount of the active form (Lim et al., 1997). Although precise regulatory pathways of MMP-9 neuronal expression remain to be established, it is possible that synaptic transmission may regulate early MMP-9 protein accumulation, whereas factors involved in tissue remodeling may initiate the mRNA upregulation and translocation as well as enzymatic activation. It is known that MMPs respond to defined factors involved in regulation of tissue morphogenesis, including neurotrophins, growth factors, and adhesion molecules. Some of these factors are expressed after kainate (Zagulska-Szymczak et al., 2001), and linking them with the MMP-9 response would be of great interest.

MMP-9 activation correlates temporally with two phenomena evoked by kainate treatment: neuronal death and remodeling. Although degradation of ECM proteins may induce neuronal loss in adult hippocampus (Chen and Strickland, 1997), there is no direct evidence for MMP-9 participation in this process. Recent results in neuronal cell cultures have shown that MMP-9 does not induce cell death (Vos et al., 2000). Moreover, in Alzheimer's disease, which is associated with significant neuronal cell loss, MMP-9 activity remained unchanged (Lim et al., 1997). Similarly, in developing cerebellum, MMP-9 activity was not elevated at the time of developmental cell death (Vaillant et al., 1999). After kainate treatment, upregulation of MMP-9 protein or mRNA was not detected in degenerating regions. Instead, the enzyme disappeared from regions undergoing cell loss (e.g., piriform cortex, amygdala, and the CA subfields) but not from the nonlesioned DG. Hence, it is unlikely that MMP-9 expression after kainate is directly associated with neuronal cell death.

DG responds to kainate in a unique way. Enhanced synaptic activity and loss of afferents from damaged limbic cortex prompt granule neurons to remodel their dendritic connections. This may be accomplished by elimination of synaptic connections with dying cortical neurons, similarly to the DG response to the piriform cortex lesion (Parnavelas et al., 1974; Matthews et al., 1976a). In addition, restoration of connections with surviving cortical neurons (Matthews et al., 1976b) or formation of synapses with sprouting mossy fibers (Cronin and Dudek, 1988; Suzuki et al., 1997; Sutula et al., 1998) may be induced. Interestingly, kainate treatment enhanced MMP-9 mRNA expression and activity in both the DG granular layer and molecular layer, the site of granule neuron dendrites. This result suggests that MMP-9 mRNA undergoes a translocation from cell body to dendrite. Dendritic trafficking of selected mRNAs is a recently discovered mechanism for the spatial control of synaptic protein expression (Steward, 1997). Translocation of MMP-9 mRNA to dendrites may allow for dendritic synthesis of this protein. This may explain the observed enhancement of diffuse protein immunostaining and gelatinase activity in the DG that we saw in some animals, without an apparent increase in the dendritic labeling, which would be expected if the protein were synthesized in the cell body and transported to terminals. Whereas the dendritic translocation of MMP-9 mRNA appears to be an especially plausible and attractive explanation for our result, one should also alternatively consider enhanced mRNA accumulation in local glia. However, we did not observe either punctate distribution of the MMP-9 within other parts of hippocampus or its upregulation in lesioned pyriform cortex, patterns that are typical for glia gene expression in neurodegeneration (Rivera et al., 1997).

The discordance that can be seen between the MMP-9 immunostaining (very subtle changes) versus extracted protein analyses (clear upregulation of the protein and activity on the Western blot and zymograms, respectively) can be explained simply by different detection thresholds of these techniques. By applying

zymography, which proved to be the most sensitive technique for MMP detection, we were able to detect clear upregulation of MMP-9 in granular and molecular layers of DG after kainate application.

Role of neuronal MMP-9 in brain functioning

Activity- and trophic factor-dependent formation and reorganization of neuronal connectivity are critical during development, adulthood cellular plasticity, and learning. These phenomena use dynamic changes in the motility and shape of neuronal processes (Matus, 2000). Acute changes can be accomplished by modulation of the existing adhesion state of the neuronal contacts (Bruses, 2000). More profound reorganizations within neuronal circuitry, such as disconnecting of dying neurons or wiring of newly formed cells, may require highly regulated proteolytic disassembly of ECM (Yamada et al., 1997; Hsueh et al., 1998; Patton et al., 1998). Our findings on the unique expression pattern of neuronal MMP-9 induced by enhanced synaptic activity and limbic system reorganization suggest that MMPs may be involved in activity-dependent regulation of the peridendritic environment with possible effects on synaptic physiology.

REFERENCES

Backstrom JR, Limm GP, Cullen MJ, Tokes ZA (1996) MMP-9 is synthesized in neurons of the human hippocampus and is capable of degrading the amyloid-β peptide (1–40). J Neurosci 16:7910–7919.

Blondel O, Collin C, McCarran WJ, Zhu S, Zamostiano R, Gozes I, Brenneman DE, McKay RD (2000) A glia-derived signal regulating neuronal differentiation. J Neurosci 20:8012–8020.

Bruses JL (2000) Cadherin-mediated adhesion at the interneuronal synapse. Curr Opin Cell Biol 12:593–597.

Chen ZL, Strickland S (1997) Neuronal death in the hippocampus is promoted by plasmin-catalyzed degradation of laminin. Cell 91:917–925.

Cronin J, Dudek FE (1988) Chronic seizures and collateral sprouting of dentate mossy fibers after kainic acid treatment in rats. Brain Res 474:181–184.

Del-Bigio MR, Jacque CM (1995) Localization of proteinase expression in the developing rabbit brain. Brain Res Dev Brain Res 86:345–347.

Gottschall PE, Deb S (1996) Regulation of matrix metalloproteinase expressions in astrocytes, microglia and neurons. Neuroimmunomodulation 3:69–75.

Hsueh YP, Yang FC, Kharazia V, Naisbitt S, Cohen AR, Weinberg RJ, Sheng M (1998) Direct interaction of CASK/LIN-2 and syndecan heparan sulfate proteoglycan and their overlapping distribution in neuronal synapses. J Cell Biol 142:139–151.

Jaworski DM (2000) Differential regulation of tissue inhibitor of metalloproteinase mRNA expression in response to intracranial injury. Glia 30:199–208.

Jaworski J, Biedermann IW, Lapinska J, Szklarczyk A, Figiel I, Konopka D, Nowicka D, Filipkowski RK, Hetman M, Kowalczyk A, Kaczmarek L (1999) Neuronal excitation-driven and AP-1-dependent activation of tissue inhibitor of metalloproteinases-1 gene expression in rodent hippocampus. J Biol Chem 274:28106–28112.

Konopka D, Szklarczyk AW, Filipkowski R, Trauzold A, Nowicka D, Hetman M, Kaczmarek L (1998) Plasticity- and neurodegeneration-linked CREM expression in the rat brain. Neuroscience 86:499–510.

Kossakowska AE, Urbanski SJ, Watson A, Hayden LJ, Edwards DR (1993) Patterns of expression of metalloproteinases and their inhibitors in human malignant lymphomas. Oncol Res 5:19–28.

Lampert K, Machein U, Machein MR, Conca W, Peter HH, Volk B (1998) Expression of matrix metalloproteinases and their tissue inhibitors in human brain tumors. Am J Pathol 153:429–437.

Lim GP, Backstrom JR, Cullen MJ, Miller CA, Atkinson RD, Tokes ZA (1996) Matrix metalloproteinases in the neocortex and spinal cord of amyotrophic lateral sclerosis patients. J Neurochem 67:251–259.

Lim GP, Russell MJ, Cullen MJ, Tokes ZA (1997) Matrix metalloproteinases in dog brains exhibiting Alzheimer-like characteristics. J Neurochem 68:1606–1611.

Matthews DA, Cotman C, Lynch G (1976a) An electron microscopic study of lesion-induced synaptogenesis in the dentate gyrus of the adult rat. I. Magnitude and time course of degeneration. Brain Res 115:1–21.

Matthews DA, Cotman C, Lynch G (1976b) An electron microscopic study of lesion-induced synaptogenesis in the dentate gyrus of the adult rat. II. Reappearance of morphologically normal synaptic contacts. Brain Res 115:23–41.

Matus A (2000) Actin-based plasticity in dendritic spines. Science 290:754–758.

Nagase H, Woessner Jr JF (1999) Matrix metalloproteinases. J Biol Chem 274:21491–21494.

Nedivi E, Hevroni D, Naot D, Israeli D, Citri Y (1993) Numerous candidate plasticity-related genes revealed by differential cDNA cloning. Nature 363:718–722.

Olson MW, Toth M, Gervasi DC, Sado Y, Ninomiya Y, Fridman R (1998) High affinity binding of latent matrix metalloproteinase-9 to the alpha2 (IV) chain of collagen IV. J Biol Chem 273:10672–10681.

Parnavelas JG, Lynch G, Brecha N, Cotman CW, Globus A (1974) Spine loss and regrowth in hippocampus following deafferentation. Nature 248:71–73.

Patton BL, Chiu AY, Sanes JR (1998) Synaptic laminin prevents glial entry into the synaptic cleft. Nature 393:698–701.

Pollard H, Charriautmarlangue C, Cantagrel S, Represa A, Rabin O, Moreau J, Ben-Ari Y (1994) Kainate induced apoptotic cell death in hippocampal neurons. Neuroscience 63:7–18.

Rivera S, Khrestchatisky M (1999) Matrix metalloproteinases and tissue inhibitors of metalloproteinases in neuronal plasticity and pathology. In: Advances in synaptic plasticity (Baudry M, Davis JL, Thompson RF, eds), pp 53–86. Cambridge, MA: MIT.

Rivera S, Tremblay E, Timsit S, Canals O, Ben-Ari Y, Khrestchatisky M (1997) Tissue inhibitor of metalloproteinases-1 (TIMP-1) is differentially induced in neurons and astrocytes after seizures: evidence for developmental, immediate early gene, and lesion response. J Neurosci 17:4223–4235.

Romanic AM, White RF, Arleth AJ, Ohlstein EH, Barone FC (1998) Matrix metalloproteinase expression increases after cerebral focal ischemia in rats: inhibition of matrix metalloproteinase-9 reduces infarct size. Stroke 29:1020–1030.

Sperk G (1994) Kainic acid seizures in the rat. Prog Neurobiol 42:1–32.

Steward O (1997) mRNA localization in neurons: a multipurpose mechanism? Neuron 18:9–12.

Sutula T, Zhang P, Lynch M, Sayin U, Golarai G, Rod R (1998) Synaptic and axonal remodeling of mossy fibers in the hilus and supragranular region of the dentate gyrus in kainate-treated rats. J Comp Neurol 390:578–594.

Suzuki F, Makiura Y, Guilhem D, Sorensen JC, Onteniente B (1997) Correlated axonal sprouting and dendritic spine formation during kainate-induced neuronal morphogenesis in the dentate gyrus of adult mice. Exp Neurol 145:203–213.

Vaillant C, Didier-Bazes M, Hutter A, Belin MF, Thomasset N (1999) Spatiotemporal expression patterns of metalloproteinases and their inhibitors in the postnatal developing rat cerebellum. J Neurosci 19:4994–5004.

Vos CM, Sjulson L, Nath A, McArthur JC, Pardo CA, Rothstein J, Conant K (2000) Cytotoxicity by matrix metalloprotease-1 in organotypic spinal cord and dissociated neuronal cultures. Exp Neurol 163:324–330.

Wang X, Jung J, Asahi M, Chwang W, Russo L, Moskowitz MA, Dixon CE, Fini ME, Lo EH (2000) Effects of matrix metalloproteinase-9 gene knock-out on morphological and motor outcomes after traumatic brain injury. J Neurosci 20:7037–7042.

Weeks JG, Halme J, Woessner Jr JF (1976) Extraction of collagenase from the involuting rat uterus. Biochim Biophys Acta 445:205–214.

Wells GMA, Catlin G, Cossins JA, Mangan M, Ward GA, Miller KM, Clements JM (1996) Quantitation of matrix metalloproteinases in cultured rat astrocytes using the polymerase chain reaction with a multicompetitor cDNA standard. Glia 18:332–340.

Werb Z (1997) ECM and cell surface proteolysis: regulating cellular ecology. Cell 91:439–442.

Woessner JF (1995) Quantification of matrix metalloproteinases in tissue samples. Methods Enzymol 248:510–528.

Yamada H, Fredette B, Shitara K, Hagihara K, Miura R, Ranscht B, Stallcup WB, Yamaguchi Y (1997) The brain chondroitin sulfate proteoglycan brevican associates with astrocytes ensheathing cerebellar glomeruli and inhibits neurite outgrowth from granule neurons. J Neurosci 17:7784–7795.

Yong WV, Power C, Forsyth P, Edwards DR (2001) Metalloproteinases in biology, pathology of the nervous system. Nat Rev Neurosci 2:502–511.

Yu Q, Stamenkovic I (2000) Cell surface-localized matrix metalloproteinase-9 proteolytically activates TGF-beta and promotes tumor invasion and angiogenesis. Genes Dev 14:163–176.

Zagulska-Szymczak S, Filipkowski R, Kaczmarek L (2001) Kainate-induced genes in the hippocampus: lessons from expression patterns. Neurochem Int 38:485–501.

Zhang JW, Deb S, Gottschall PE (1998) Regional and differential expression of gelatinases in rat brain after systemic kainic acid or bicuculline administration. Eur J Neurosci 10:3358–3368.

Zuo J, Ferguson TA, Hernandez YJ, Stetler-Stevenson WG, Muir D (1998) Neuronal matrix metalloproteinase-2 degrades and inactivates a neurite-inhibiting chondroitin sulfate proteoglycan. J Neurosci 18: 5203–5211.